Jurnal
Teknologi

Full Paper

MECHANICAL PROPERTIES OF POLYSULFONE-ZnO NANOCOMPOSITE MEMBRANE

Malikhatul Hidayah[a,c], Tutuk Djoko Kusworo[a,b]*, Heru Susanto[a,b]

[a]Department of Chemical Engineering, Faculty of Engineering, Diponegoro University, Semarang, Indonesia, 50275
[b]Membrane Research Center (Mer-C), Integrated Laboratory, Diponegoro University, Semarang, Indonesia, 50275
[c]Chemistry Department, Faculty of Science and Technology, Walisongo State Islamic University, Semarang, Indonesia, 50181

Article history
Received
12 January 2021
Received in revised form
4 May 2021
Accepted
23 May 2021
Published online
20 June 2021

*Corresponding author
tdkusworo@che.undip.ac.id

Graphical Abstract

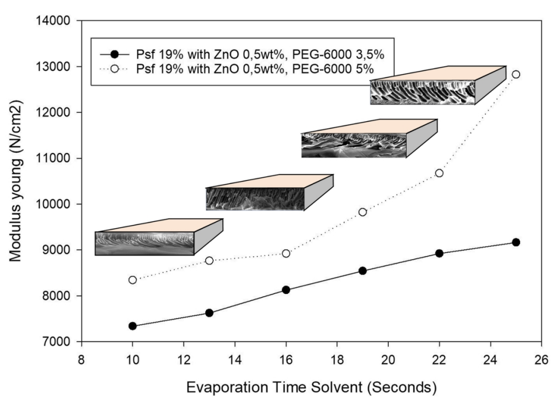

Abstract

Large quantities of wastewater are generated by the petroleum refining process. Micron-scale emulsion droplets and submicron droplets are difficult to remove from oil-refined wastewater, and addressing these issues has been a major challenge for researchers. Membrane technology is widely used in water treatment because it is very selective and effective in the filtration process. This research focuses on oil refinery water treatment using a polysulfone membrane (PSF)-nano-ZnO membrane with the addition of polyethylene glycol (PEG). This research aims to determine the PEG ratio that produces the optimum PSF-ZnO membrane in terms of mechanical properties, including thickness, tensile strength, and molecular weight cut off (MWCO) value. The membrane with the optimum clearance was obtained at 3% PEG with a thickness of 0.0077 mm, Young's modulus of 8800 N/m^2, and Morphological analysis was performed using the SEM (Scanning Electron Microscopy) method on the membrane which had the highest and lowest permeability values. The best membrane MWCO value was achieved by the addition of 19% PSF-nano-ZnO 1% wt at 5 minutes of UV irradiation. This shows that the addition of PEG composite affects pore openings. The membrane formed with variations in PEG concentrations effecting the thickness of the membrane. Higher concentrations make the membrane thicker, resulting in a higher Young's modulus.

Keywords: Membrane, PSF-ZnO, PEG, tensile strength, thickness

1.0 INTRODUCTION

The increasing consumption of oil and gas is currently causing a large amount of wastewater in oil refineries [1] appropriate technology is developed to obtain clean water. The water that comes out of the oil refinery waste can be processed through appropriate technologies that can remove harmful contaminants [2]. Therefore, the main task of wastewater treatment is to remove harmful contaminants so that treated wastewater can be disposed of properly or can be reused [3]. It is estimated that by 2040 world oil demand will increase rapidly, and refinery wastewater purification should be of increasing concern [4]. because petroleum production activities and processes produce significant amounts of wastewater. This wastewater comes from oil drilling and refining, and it produces a flow of organic-inorganic compositions and concentrations that vary with the ability of the camp to migrate downstream, resulting in air and soil pollution or spill over to the air surface causing a large-scale environmental problem [5]. Appropriate treatment is needed to make oil refinery wastewater usable properly, which relates to costs, work methods, safety, and time efficiency in obtaining clean water that is acceptable to the community. Some common waste processing technologies, such as existing pre-treatment methods, include air flotation, hydrocyclones, coalescer beds, and filtration. However, these methods are less effective because they create offensive odours, the tools and materials are expensive, a large space is required, and they take a long time [6].

Currently, the most profitable wastewater treatment system uses membrane technology, because it can reduce organic-inorganic compounds in wastewater without any chemical changes in operation [7]. In addition to saving energy, membrane processes also offer the advantages of compactness, light weight, and high productivity that puts this process in perfect harmony with the process intensification strategy [8]. In this study, a polysulfone (PSF) membrane material is used. This membrane is widely used in water treatment because it exhibits high resistance, bacterial resistance, heat resistance, and excellent chemical thermal and mechanical strength stability over a large pH range [9]. However, there are several drawbacks of membrane technology, including capital and cost of fabrication, antifouling, packing density, and scalability [10].

Good membrane, obtained from the selection of materials Based on the structure, oil refinery waste water which contains organic and inorganic materials which are considered as B3 (Toxic and Hazardous Materials) waste which affects the environment and human health [11]. This water can pollute the environment, the environment cannot be maintained properly. One of the alternative technologies that can be used for processing oil refinery wastewater is membrane technology that can be used as a new water source for agricultural irrigation, industrial water, and drinking water [12]. This type membrane of asymmetric membrane is generally used for ultrafiltration due to its strong mechanical qualities. Parameters related to the membrane formation mechanism on the shape and performance characterization of the membrane include the influence of concentration in printing [13] and the thickness of the membrane. These parameters affect the demixing process that occurs either instantaneously or slowly in the coagulation tub [14]. The thickness test on the membrane effect of variations in the composition of the membrane constituents in the same unit area [15]. In addition to the thickness test, a tensile test is also needed, one of the tensile tests (mechanical stress) aims to determine the mechanical strength of the membrane against the force exerted by the environment [16]. This test describes the tensile strength/elasticity of a membrane. The membrane is said to be elastic if the membrane has a high tensile strength when a certain amount of force is applied to it. An elastic membrane will be advantageous over a membrane that is easily cracked (fragile) [17]. Therefore, this research focuses on the morphology, thickness, and tensile strength of PSF-Nano-ZnO membranes. Modifications were made to achieve high selectivity in the processing of oil refinery wastewater.

2.0 METHODOLOGY

Materials

PSF (UDEL®PSU) is a membrane material from Solvay Advanced Materials, USA. N-methyl-2-pyrrolidone (NMP) was purchased from Merck, USA as a polymer solvent. Inorganic nano-ZnO additives were supplied by Nano Center Indonesia, Indonesia. Polyvinyl alcohol (PVA) as a surface modifier additive and polyethylene glycol (PEG) 6000 Da and 4000 Da as a porogen agent were obtained from Merck, USA. Refinery samples were obtained from petroleum factories (Pertamina, Ltd., Indonesia) with the following initial characteristics: TDS up to 888 mg/L, COD up to 227.6 mg/L, and ammonia up to 48.2 mg/L. Furthermore, pisaucasting (254 µm) and glass plates were used to make membranes, and dead-end ultrafiltration modules were used in filtration performance tests.

PSF-Nano ZnO Composite Membrane Fabrication

The membrane is made through phase inversion, which is a process of changing the form of a polymer from a liquid phase to a solid under controlled conditions. PSF-ZnO dope solution solidification begins with the transition from the first liquid phase to the second liquid phase (liquid-liquid demixing). 19% PSF, 0.5% nano ZnO, and 5% PEG using NMP solvent.

The manufacturing stage of the polyethersulfone (PSf)-nano-ZnO ultrafiltration membrane starts by making a PSF printing solution consisting of 19 wt% in total solids with ZnO compositions of 0,5 wt %, 1 wt %, and 1,5 wt %, with NMP solvent 80 wt % of total solids. Membrane printing was done using a glass plate and a pouring knife. Before being immersed in the coagulation bath, it was first irradiated with UV for 1 minute, 5 minutes, and 10 minutes. The glass plate is immersed in a coagulation bath. The printed membrane is then left for 1 day in clean water. The membrane is then dried at atmospheric temperature for 1 day.

Furthermore, in the next stage, characterization was carried out by scanning electron microscopy or SEM. After that, the membrane thickness and tensile strength tests for processing oil refinery wastewater are carried out.

Table 1 variable influence for PSf-nano ZnO

RUN	Variabel				
	Polymer Concentration (wt%)	Concentration of nanoZnO (wt%)	Addition of PEG (specific gravity) + NMP 80%	UV irradiation time (minute)	Addition of PVA (wt%)
1		0,5			
2	19	1	-	-	-
3		1,5			
4	19	Best concentration	4000	-	-
5			6000		
6		Best concentration		1	
7	19		Best weight	3	-
8				5	
9		Best concentration			1
10	19		Best weight	Best time	2
11					3

Determination of Morphological Membrane Structure

This study used the SEM test to determine a morphological picture of the membrane. With this test, the surface structure and cross-section of a polymer can be seen using an electron microscope [18]. SEM analysis used a Hitachi S5500 microscope. The membrane surface was analysed by an atomic force microscope [30]. This study used the SEM test to determine a morphological picture of the membrane. With this test, the The membrane is made small and put into liquid nitrogen. Then, the sample is dried. The dry sample was given a carbon spray to make it conducive, prior to SEM analysis [19]. The advantages of SEM are knowing the pore distribution, pore geometry, pore size, and porosity on the surface [20].

Membrane Characterization Using a Thickness Test

Membrane thickness measurements are very useful for both membrane users and manufacturers because membrane thickness is an indirect indicator of uniformity and quality [21]. Measurement of membrane thickness can be done by a micrometer; it is measured at random locations and the average thickness is calculated. Furthermore, increasing the membrane thickness can increase energy efficiency up to asymptotic values [22].

Membrane Characteristics Using the Tensile Test

In this study, the measurement of mechanical properties used a tensile test with a texture analysis tool. From the tensile test results get Young's modulus value. This test is done by pulling the membrane until it breaks. Then, Young's modulus is obtained. A tensile test is one of the physical property tests that involve deformation of a material under certain stress. Mechanical strength and membrane stability were evaluated using an atenyl testing machine. Then the mechanical length is determined using a tensile testing machine to produce Young's modulus and determine the stability of the membrane [23]. The tensile strength and elongation tests in this study used a Universal Testing Machine. Film specimens were cut (8 cm x 0.5 cm) from each sample and fixed between the machine grips. Mathematically, this relationship can be formulated as Equation 1.

$$Tensile\_strength\left(N/m^2\right) = F/A \qquad (1)$$

Information:
F: tensile strength (N)
A: cross-sectional area (m²)

Determination of Contact Angle

When a liquid or gas is exposed to a solid, they will come into contact with one another. The contact angle describes the interaction between the liquid and the surface of a solid object which can be known through the shape of the fluid that is on the surface of the solid object [24]. A schematic of the contact angle is shown in Figure 1.

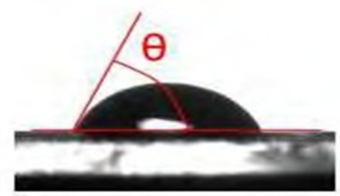

Figure 1 Fluid contact angle

In the test, the membrane contact angle was determined using the Goniometer technique. The sample was brought into contact with ionized water as a contact between the water and the sample [25]. The data on the results of the PSF-ZnO membrane sample were taken from the average contact angle value of the ten measured points.

Determination of the Amount of Wastewater Absorbed by the Membrane

The porosity test is carried out to determine the amount of substances or components that can be absorbed by the membrane. The membrane porosity test is usually carried out on water. The method used for the porosity test is to immerse the membrane in water for 1 day at standard room temperature, then the membrane is weighed [26], the amount of membranee porosity by Equation 2.

$$porosity = \frac{\left(w_{wet} - w_{dry}\right)}{w_{dry}} \times 100\% \qquad (2)$$

where: w wet is heavy wet, w dry is heavy dry and the proportion of membrane volume weight (%)

Molecular Weight Determination

MWCO is the limit of molecular weight values that the membrane can hold, namely with a % R-value above 90. An MWCO value of 50 means that the membrane can hold a molecule with a weight of 50,000 to 90% or more [27]. The MWCO value is obtained from the graph of % PEG rejection of the molecular weight value. In MWCO characterization, the solute molecular weight is used as a standard, which is usually dextran or PEG. Experiments were carried out by permeating the membrane with various molecular weights of dextran solutions. The dextran solutions had molecular weights of 400, 4000, 6000, and 10,000 Daltons. The concentration of the dextran solution used GPC [28].

3.0 RESULTS AND DISCUSSION

SEM Characterization of Fabricated Membrane

SEM is used to see membrane morphology, surface state and membrane sublayer relationships by looking at the membrane cross-section [29]. SEM analysis was performed using a Hitachi S5500 microscope The topology of the membrane surface was examined using atomic force microscopy analysis. The results of membrane characterization aree presented in Figure 2.

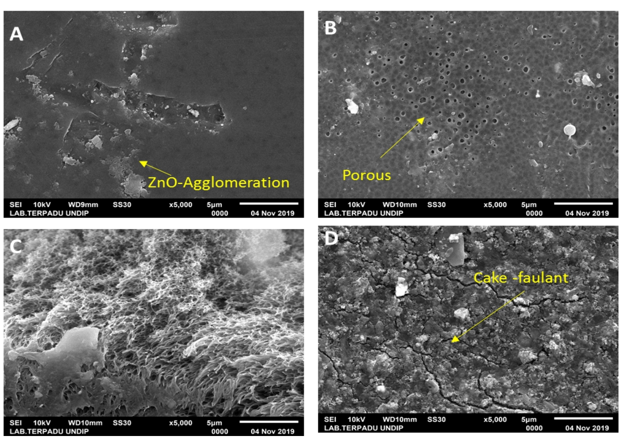

Figure 2 Morphology A) PSF-nano-ZnO membrane surface, B) PSF-nano-ZnO membrane surface with 6000 Da PEG and 1 min UV (before filtration), C) PSF-nano-ZnO cross-section with 6000 Da PEG and 1 min UV, D) Surface PSF-nano-ZnO membrane with 6000 Da PEG and 1 min UV (after filtration)

Figure 2A shows the surface of the PSF-nano-ZnO membrane without modification. The surface looks smoother and there are no visible pores, compared to Figure 2B. Figure 2B shows a membrane surface that has been modified by adding PEG 6000 Da additive and UV irradiation for 1 minute. This phenomenon explains that PEG and UV irradiation affect the membrane that PEG can be used for pore-forming [31]. The surface pores are clearly visible, and the roughness increases with an increase in the PEG molecular weight. UV irradiation was carried out to avoid agglomeration [32], but in Figure 2A, it appears that agglomeration occurs with many lumps on the surface. Thus, UV irradiation of the membrane results in increased pore sizes. The presence of PEG and UV irradiation can also form like cavities between the sub-layers of the membrane surface and large voids at the bottom of the membrane, as shown in Figure 2C and 3C. Furthermore, the 2D image shows a PSF-nano-ZnO membrane with 6000 Da PEG and 1 minute of UV irradiation after being used for filtration The figure shows that the occurrence of cake occurs on the membrane surface due to contaminants in the liquid waste accumulating on the membrane surface. However, it is different in Figure 3C which does not experience a buildup of contaminants on the membrane surface. Figure 3C is a membrane that has used PVA. These results confirm that PVA can increase anti-fouling on membranes compared to membranes without PVA.

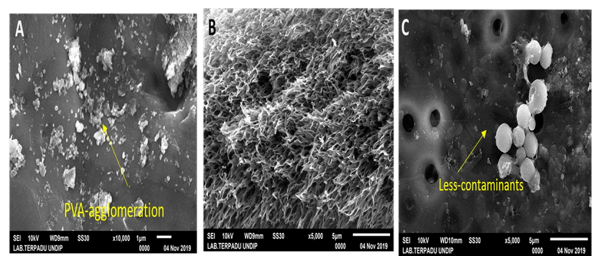

Figure 3 Morphology (A) The surface of the PSf-nanoZnO membrane with the addition of PVA, (B) Cross-section of the PSf-nanoZnO membrane with the addition of PVA (Before filtration), (C) Surface of the PSf-nanoZnO membrane with the addition of PVA (After filtration)

The Effect of PVA Modification on FTIR Characterization

The next characterization is FT-IR, which is used to see the membrane spectrum so that the functional groups can be defined. The FT-IR distribution is shown in Figure 3.

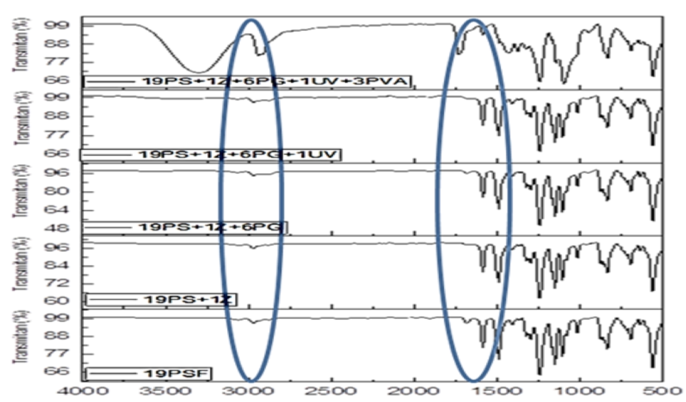

Figure 4 The FT-IR spectrum of PSf-nano ZnO membrane with various modifications

Figure 4 shows the frequency of the PSf-nano ZnO membrane with multiple changes. Intense absorption at wavelengths of 1280 and 1326 cm^{-1}, symmetrical strain vibration O=S=O coming from pure PSf as the main chain in the membrane matrix. The two-wavelength peaks of 1366 and 1489 cm^{-1} correspond to the symmetrical deformation vibrations and the asymmetrical deformation vibrations of-OH, respectively. The observed absorption rate was 1586 cm^{-1}. Meanwhile, the wavelength of 3000 cm^{-1} shows asymmetrical stretching vibration -CH [33]. Furthermore, the 1756 cm^{-1} region's wavelength changed after adding 1% wt% nano ZnO, which proved the existence of OH stretch due to the presence of ZnO. This phenomenon show indicates a cross-linking of the PVA-nano ZnO matrix membrane and PVA. The absorption shows strong water adsorption because the peak is O-H in the PVA [34]. Nevertheless, the modification of the Psf-nano ZnO membrane did not change the main membrane matrix chain. This phenomenon shows that the membrane produced is stable.

Thickness Test Results

The thickness of the film was measured using a micrometer (accuracy 0.001 mm) by placing the film between the micrometer jaws., membrane thickness was measured at five different points, then averaged [35]. The average membrane thickness using different PEG concentrations can be found in Figure 5.

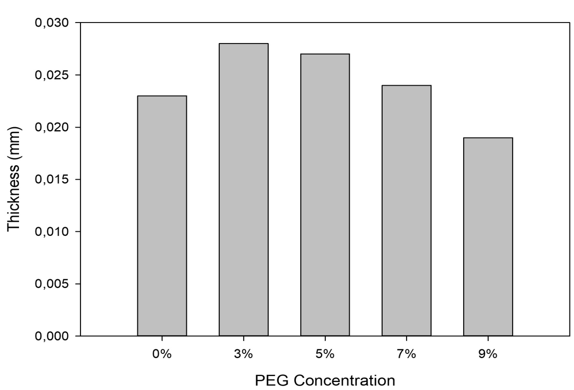

Figure 5 Relationship between PEG concentration and membrane thickness

Membranes formed with various PEG concentrations had various thicknesses. The mean thickness measurements (Figure 5) show that increasing the PEG concentration increases the thickness. The highest membrane thickness was 0.028 mm at a PEG concentration of 3%, and the lowest was 0.0023 mm at a PEG concentration of 0%. This membrane is thinner than the polymer-based membrane (0.0167 mm) [36]. The membrane thickness can influence membrane filtration characterization. This phenomenon explains that PEG and UV irradiation affect the membrane. [37] stated that PEG can be used as a pore former. The surface pores were clearly visible, and the roughness increased with the addition of higher molecular weights of PEG.

Evaluation of Mechanical Strength

High quality membranes have good mechanical properties. Young's modulus can be increased by increasing the ZnO concentration [38]. From Figure 5, solvent evaporation affects the characteristics of the membrane, and as evaporation time increases, the mechanical strength of the membrane increases.

The longer the solvent evaporation time, the tighter the pores of the membrane and the higher the ZnO concentration, so that the membrane thickens and Young's modulus increases. This is because a thicker membrane has stronger polymer bonds and is more difficult to break. Additionally, the SEM results show that the quantity of macrovoids, such as fingers, at an evaporation time of 25 seconds is less than at 10 seconds. Large macrovoids reduce the mechanical strength, resulting in a smaller modulus in the membrane.

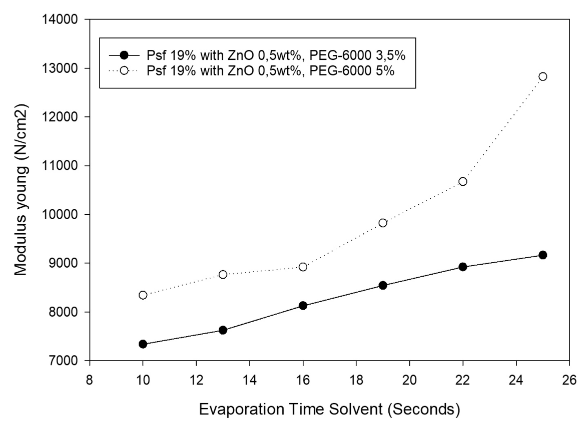

Figure 6 Young's modulus of the PSF-ZnO membrane with variations in liquid PEG and variations in the time of solvent evaporation

Figure 7 shows that the addition of 1% distilled water increases Young's modulus; this is due to the hydrogen bonds causing the membrane to become plastic. The pores are denser and the mechanical properties are stronger and more resistant to pressure.

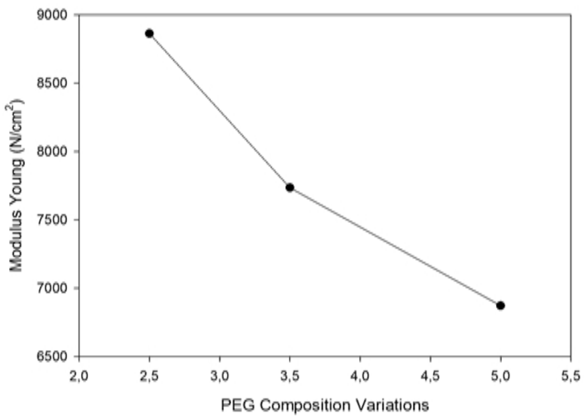

Figure 7 Young's modulus with variations in the composition of the dope of 2.5%, 3.5%, and 5% liquid PEG, 19% PSF, and 25 seconds of solvent evaporation time

Figure 7 shows that the higher the PEG concentration, the lower Young's modulus. This is because PEG can reduce hydrogen bonds and form soft segments, causing its mechanical properties to degrade. The higher the PEG concentration, the weaker the mechanical properties, because the membrane becomes smoother and softer.

Contact Angle Test

The results of the contact angle test are shown in Figure 7. The contact angles are divided into three categories, namely (1) Large contact angles (> 90°) hydrophilic; (2) Small contact angles (< 90°) hydrophobic (3) Very small contact angles (< 0°) Superhydrophilic.

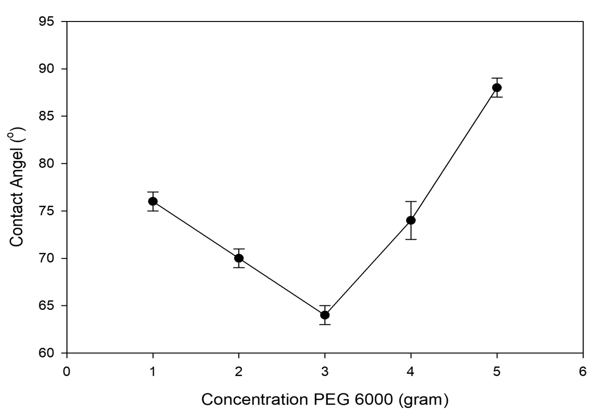

Figure 9 Relationship between the concentration of PEG 6000 and the angle of contact

In Figure 7, the concentration of PEG 6000 added to the PSF-nano-ZnO membrane composite affects of the contact angle. The addition of PEG 6000 reduced the contact angle to its lowest value at a PEG 6000 concentration of 2 grams and then increased again with increasing PEG 6000 concentrations. According to [39] the Cassie Effect can state that when the print solution is immersed in a coagulant bath, additives which are missible with the non-solvent in the coagulant bath, immediately diffuse out of the resulting solution to the solid membrane. The addition of these fillers has the effect of increasing the surface hardness and hydrophobicity of the membrane [40]. This Cassie effect is because, when the casting solution is in the coagulant bath, any additive that cannot be dissolved with the non-solvent will diffuse out of the print solution to produce a solid membrane. The greater the PEG 6000 concentration added to the printing solution, the faster the diffusion that occurs. As a result, the process of compaction of the print solution resulted in a larger pore in the addition of PEG 6000 with a greater concentration. However, with the addition of PEG 6000 in 3- and 4-gram concentrations, the pore size decreased. This is because the diffusion of the filler, namely PEG 6000, when immersed in the coagulation bath, runs quickly, while on the membrane surface there is still trapped air. This causes the surface membrane to dry out, resulting in higher surface roughness. This explanation proves that the Cassie effect can decrease the membrane contact angle with increasing surface roughness.

The Cassie effect causes the contact angles of the PSF membranes with PEG 6000 concentrations of 3 grams and 4 grams to increase. Therefore, the best PSF membrane contact angle is at a PEG 6000 concentration of 2 grams. The results of the digital contact angle test in Figure 3.4 show that complete wetting is on the membrane with a PEG 6000 concentration of 2 grams. Perfect wetting can make the resulting contact angle the smallest. Decreased contact angle values and the Cassie effect due to increased hydrophilicity [41]. As the filler increases, the contact angle decreases and the membrane surface roughness increases, according to the Cassie effect. Study [42] came to the same conclusion. The results of the contact angle test showed that contact angles decreased with increasing concentration but increased again when the PSF concentration was greater. This increase is due to the surface roughness becoming more dominant and decreasing the membrane hydrophilicity. The rougher the membrane surface, the greater the value of the contact angle.

Membrane Porosity Test

A porosity test was performed to determine the amount of substance that can be absorbed by the membrane. The porosity test in this study was carried out using water. The membrane porosity value is calculated using the formula in Equation 2, and the results are shown in Figure 8.

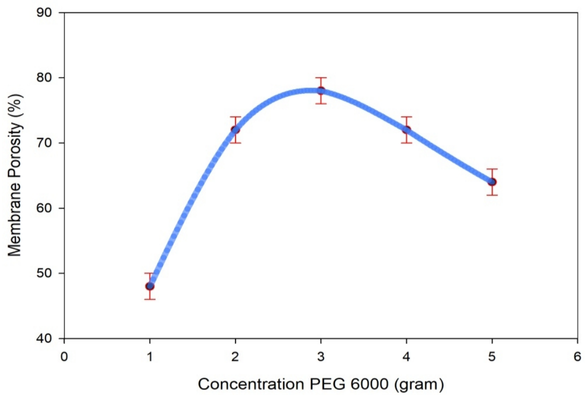

Figure 10 Relationship between PEG 6000 concentration and membrane porosity

Figure 9 shows the porosity test results for the PSF-nano-ZnO membrane. The addition of PEG 6000 can increase membrane porosity; however, the addition of too much additive resulted in a decrease in membrane porosity. the increasing concentration of PEG 6000 caused the membrane porosity to increase significantly [43]. However, when the addition of PEG 6000 was continued, the phase separation on the membrane was delayed, resulting in lower porosity. Thus, the best porosity was on the PSF membrane with a PEG 6000 concentration of 2 grams, namely 78.863%.

The results of membrane porosity are in accordance with study [44], which showed increased porosity with the addition of additives up to 2 grams, and a decrease in porosity when the addition was continued. Increased porosity due to the addition of PEG can enlarge the pores so that the porosity increases. However, if the additive concentration is even higher, the PEG will be agglomerated, thus minimizing the pores that have been formed. Likewise, study [45] shows the same membrane porosity pattern. The addition of additives at low concentrations will be able to increase porosity because the additives can diffuse completely and form larger pores. However, when the additive is added at a high concentration, the additive will agglomerate and not diffuse completely so that the pore sizes become smaller. This porosity can be shown in the morphology of the formed membrane.

Measurement of MWCO Membranes Final Membrane Analysis with MWCO

MWCO is a weight value limit that can be retained by the membrane with an R-value above 90%. The MWCO value for the membrane as the polymer concentration increases for each membrane gives the molecular weight of the dextran. The smaller the membrane pores formed, the smaller the membrane MWCO value. This applies to the three types of membrane polymers.

The MWCO dextran rejection of PSF-ZnO can be seen in Figure 3. This study used a dextran solution with molecular weight variations of 400, 4000, 6000, and 10,000 Da. The results of MWCO experiments for 19% PSF membrane, PES 19% nano-ZnO 1% wt with UV 1 minute, and PSF 19% nano-ZnO 1% wt with UV 5 minutes, are shown in Figure 9.

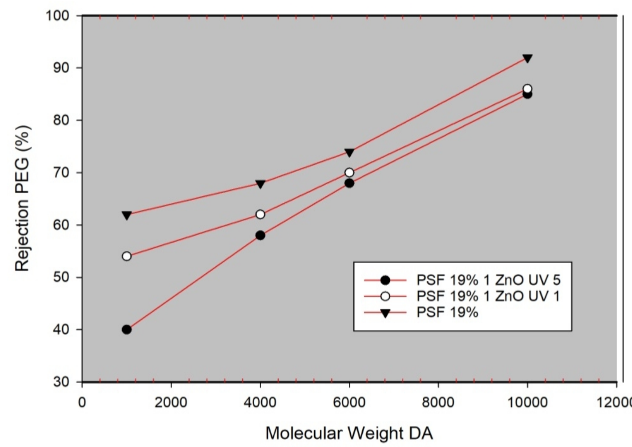

Figure 10 Comparison of molecular dextran weight with PEG rejection

The figure shows that the MWCO value on the PSF-Nano-ZnO membrane without the addition of particles has the lowest value. Porosity is a measure of the empty spaces, or voids, on the membrane. It is different on the PSF membrane with the addition of ZnO nanoparticles having higher porosity values so that the flux becomes high [46]. The addition of UV also gives it a higher porosity value, which makes the flux value even higher.

4.0 CONCLUSIONS

In this study, to obtain the best mechanical membrane properties (thickness, tensile strength, and MWCO value), compositions of PEG were added to alter the order and pores of the membrane. This increase can be predicted by the roughness and the aggregate size on the membrane surface, and a 3% PEG concentration can increase the membrane thickness. Measurement of the mechanical properties of the membrane was carried out using a tensile test with a texture analyser. From the thickness test results of 0.0077 mm thickness, 8800 N/m^2 Young's modulus, and SEM results of the membrane at 25 seconds of evaporation time at the membrane contact angle with a PEG 6000 concentration of 2 grams, the best membrane MWCO value was achieved with the addition of PSF 19% nano-ZnO 1% wt with 5 minutes of UV irradiation. The longer the time for the evaporation of the solvent to produce a membrane with tight pores (because when the solvent is evaporated the liquid polymer solution moves to fill the pores, resulting in denser pores), the higher the Young's modulus.

Acknowledgement

The authors gratefully acknowledge the facility support from the Waste Management Laboratory of the Chemical Engineering Department.

References

[1] Wang, Y., Wang, Q., Li, M., Yang, Y., He, W., Yan, G., *et al.* 2016. An Alternative Anaerobic Treatment Process for Treatment of Heavy Oil Refinery Wastewater Containing Polar Organics. *Biochem Eng J*. 105: 44-51. Available from: http://dx.doi.org/10.1016/j.bej.2015.08.012.

[2] Hernández-francisco, E., Peral, J., Blanco-jerez, L. M. 2017. Removal of Phenolic Compounds from Oil Refi Nery Wastewater by Electrocoagulation and Fenton / photo-Fenton Processes. *J Water Process Eng*. 19(February): 96-100. Available from: http://dx.doi.org/10.1016/j.jwpe.2017.07.010.

[3] Khouni, I., Louhichi, G., Ghrabi, A., Moulin, P. 2020. Efficiency of a Coagulation/flocculation–membrane Filtration Hybrid Process for the Treatment of Vegetable Oil Refinery Wastewater for Safe Reuse and Recovery. *Process Saf Environ Prot*. 135: 323-41. Available from: https://doi.org/10.1016/j.psep.2020.01.004.

[4] Sharma, S., Simsek, H. 2019. Chemosphere Treatment of Canola-oil Refinery Effluent using Electrochemical Methods : A Comparison between Combined Electrocoagulation þ Electrooxidation and Electrochemical Peroxidation Methods . *Chemosphere*. 221: 630-9. Available from: https://doi.org/10.1016/j.chemosphere.2019.01.066.

[5] Abass, O. K., Fang, F., Zhuo, M., Zhang, K. 2018. Science of the Total Environment Integrated Interrogation of Causes of Membrane Fouling in a Pilot-scale Anoxic-oxic Membrane Bioreactor Treating Oil Refinery Wastewater. *Sci Total Environ*. 642: 77-89. Available from: https://doi.org/10.1016/j.scitotenv.2018.06.049.

[6] Alexandre, V. M. F., de Castro, T. M. S., de Araújo. L. V., Santiago, V. M. J., Freire, D. M. G., Cammarota, M. C. 2016. Minimizing Solid Wastes in an Activated Sludge System Treating Oil Refinery Wastewater. Chem Eng. *Process Process Intensif*. 103: 53-62. Available from: http://dx.doi.org/10.1016/j.cep.2015.10.021.

[7] Samaei, S. M., Gato-trinidad, S., Altaee, A. 2018. The Application of Pressure-Driven Ceramic Membrane Technology for the. *Sep Purif Technol*. Available from: https://doi.org/10.1016/j.seppur.2018.02.041.

[8] Ali, A., Tufa, R. A., Macedonio, F., Curcio, E., Drioli, E. 2018. Membrane Technology in Renewable-energy-driven Desalination. *Renew Sustain Energy Rev*. 81(July 2017): 1-21. Available from: http://dx.doi.org/10.1016/j.rser.2017.07.047.

[9] Costa, J. B., Lima, M. J., Sampaio, M. J., Neves, M. C., Joaquim, L., Morales-torres, S. *et al.* 2018. Enhanced Biocatalytic Sustainability of Laccase by Immobilization on Functionalized Carbon Nanotubes / Polysulfone Membranes. *Chem Eng J*. Available from: https://doi.org/10.1016/j.cej.2018.08.178.

[10] Sarihan, A., Eren, E., Eren, B., Erdo, Y. 2019. Flux-enhanced Polysulfone Membranes Blended with ABPBI as a Novel Additive. 20(August): 6-11.

[11] Hua, F. L., Tsang, Y. F., Wang, Y. J., Chan, S. Y., Chua, H., Sin, S. N. 2007. Performance Study of Ceramic Microfiltration Membrane for Oily Wastewater Treatment. *Chemical Engineering Journal.* 128(2-3): 169-75. DOI: 10.1016/j.cej.2006.10.017.

[12] Dami, S., Abetz, C., Fischer, B., Radjabian, M., Georgopanos, P., Abetz, V. 2017. A Correlation between Structural Features of an Amphiphilic Diblock Copolymer in Solution and the Structure of the Porous Surface in an Integral Asymmetric Membrane. *Polymer.* 126: 376-85. DOI: 10.1016/j.polymer.2017.05.024.

[13] Ye, W., Lin, J., Borrego, R., Chen, D., Sotto, A., Luis, P. 2018. Separation and Purification Technology Advanced Desalination of Dye / NaCl Mixures by a Loose Nano Filtration Membrane for Digital Ink-jet Printing. *Sep Purif Technol*. 197(November 2017): 27-35. Available from: https://doi.org/10.1016/j.seppur.2017.12.045.

[14] Li, J., Wei, M., Wang, Y. 2017, NU SC State Key Laboratory of Materials-Oriented Chemical Engineering, Jiangsu National Synergetic. *Chinese J Chem Eng*. Available from: http://dx.doi.org/10.1016/j.cjche.2017.05.006.

[15] Iawa, I. 2016. Intervessel PIt Membrane Thickness as a key Determinant of Embollsm Resistance in Anglosperm Xylem. *IAWA J*. 37(2): 152-71.

[16] Khalifa, A., Lawal, D., Antar, M., Khayet, M. 2015. Experimental and Theoretical Investigation on Water Desalination using Air Gap Membrane Distillation. *DES*. 376: 94-108. Available from: http://dx.doi.org/10.1016/j.desal.2015.08.016.

[17] Munirasu, S., Banat, F., Ahmed, A., Abu, M. 2017. Intrinsically Superhydrophobic PVDF Membrane by Phase Inversion for Membrane Distillation. *Desalination*. 417(April): 77-86. Available from: http://dx.doi.org/10.1016/j.desal.2017.05.019.

[18] Garcia-ivars, J., Iborra-clar, M., Alcaina-miranda, M. 2016. Surface Photomodification of Flat-sheet PES Membranes with Improved Antifouling Properties by Varying UV Irradiation Time and Additive Solution pH. *Chem Eng J*. 283: 231-42. Available from: http://dx.doi.org/10.1016/j.cej.2015.07.078

[19] Yang, M., Zhao, C., Zhang, S., Li, P., Hou, D. 2017. Applied Surface Science Preparation of Graphene Oxide Modified Poly (m-phenylene isophthalamide) Nanofiltration Membrane with Improved Water Flux and Antifouling Property. *Appl Surf Sci*. 394: 149-59. Available from: http://dx.doi.org/10.1016/j.apsusc.2016.10.069.

[20] Pang, R., Li, X., Li, J., Lu, Z., Sun, X., Wang, L. 2014. Preparation and Characterization of ZrO_2/PES Hybrid Ultrafiltration Membrane with Uniform ZrO2 Nanoparticles. *Desalination*. 332(1): 60-6.

[21] Eykens, L., Hitsov, I., Sitter, K. De, Dotremont, C., Pinoy, L., Nopens, I. *et al.* 2015. Author's Accepted Manuscript. *J Memb Sci*. Available from: http://dx.doi.org/10.1016/j.memsci.2015.07.037.

[22] Prince, J. A., Bhuvana, S., Boodhoo, K. V. K., Anbharasi, V., Singh, G. 2014. Synthesis and Characterization of PEG-Ag Immobilized PES Hollow Fiber Ultrafiltration Membranes with long Lasting Antifouling Properties. *J Memb Sci*. 454: 538-48. Available from: http://www.sciencedirect.com/science/article/pii/S037673881301003X.

[23] Behboudi, A., Jafarzadeh, Y., Yegani, R. 2017. Polyvinyl Chloride/polycarbonate Blend Ultrafiltration Membranes for Water Treatment. *J Memb Sci*. 534(April): 18-24. Available from: http://dx.doi.org/10.1016/j.memsci.2017.04.011.

[24] Xu, Z., Liao, J., Tang, H, Li, N. 2018. Antifouling Polysulfone Ultrafiltration Membranes with Pendent Sulfonamide Groups. *J Memb Sci*. 548(November 2017): 481-9. Available from: https://doi.org/10.1016/j.memsci.2017.11.064.

[25] Omidvar, M. *et al.* 2015. Preparation of Hydrophilic Nanofiltration Membranes for Removal of Pharmaceuticals from Water. *Journal of Environmental Health Science and Engineering.* 13(1): 1-9. Doi: 10.1186/s40201-015-0201-3.

[26] Fan, X., Su, Y., Zhao, X., Li, Y., Zhang, R., Ma, T. 2016. Manipulating the Segregation Behavior of Polyethylene

Glycol by Hydrogen Bonding Interaction to Endow Ultrafiltration Membranes with Enhanced Antifouling Performance. J *Memb Sci*. 499: 56-64. Available from: http://dx.doi.org/10.1016/j.memsci.2015.10.026.

[27] Dehghan, R., Barzin, J. 2020. Development of a Polysulfone Membrane with Explicit Characteristics for Separation of Low Density Lipoprotein from Blood Plasma. *Polym Test.* 85(February): 106438. Available from: https://doi.org/10.1016/j.polymertesting.2020.106438.

[28] Chen, W., Wei, M., Wang, Y. 2017. Advanced Ultrafiltration Membranes by Leveraging Microphase Separation in Macrophase Separation of Amphiphilic Polysulfone Block Copolymers. *J Memb Sci.* 525(November 2016): 342-8. Available from: http://dx.doi.org/10.1016/j.memsci.2016.12.009.

[29] Khan, A, Sherazi, T. A., Khan, Y., Li, S., Ali, S., Naqvi, R. 2018. Fabrication and Characterization of Polysulfone / Modified Nanocarbon Black Composite Antifouling Ultrafiltration Membranes. 554(January): 71-82.

[30] Habibi, S., Nematollahzadeh, A. 2016. Enhanced Water Flux through Ultrafiltration Polysulfone Membrane Via Addition-Removal of Silica Nano-Particles. *Synthesis and Characterization.* 43556: 1-9.

[31] Kusworo, T. D., Aryanti, N., Qudratun, Utomo, D. P., Widayat. 2019. Improvement in Nano-hybrid Membrane PES–nanosilica Performance using Ultra Violet Irradiation and Acetone–ethanol Immersion for Produced Water Treatment. *Int J Environ Sci Technol.* 16(2): 973-86. Available from: https://doi.org/10.1007/s13762-018-1718-7.

[32] Dzinun, H. *et al.* 2017. Performance Evaluation of Co-extruded Microporous Dual-layer Hollow Fiber Membranes using a Hybrid Membrane Photoreactor. *Desalination.* 403: 46-52. Doi: 10.1016/j.desal.2016.05.029.

[33] Ezer, N., Sahin, I., Kazanci, N. 2017. Vibrational Spectroscopy Alliin interacts with DMPC Model mMembranes to Modify the Membrane Dynamics : FTIR and DSC Studies. *Vib Spectrosc*. 89: 1-8. Available from: http://dx.doi.org/10.1016/j.vibspec.2016.12.006.

[34] Ahmad, A. L., Sugumaran, J., Shoparwe, N. F. 2018. Antifouling Properties of PES Membranes by Blending with ZnO Nanoparticles and NMP-acetone Mixture As Solvent. *Membranes (Basel)*. 8(4): 1-13.

[35] Kusworo, T. D., Aryanti, N., Utomo, D. P. 2018. Oilfield Produced Water Treatment to Clean Water Using Integrated Activated Carbon-Bentonite Adsorbent and Double Stages Membrane Process. *Chem Eng J*. Available from: https://doi.org/10.1016/j.cej.2018.04.136.

[36] Shi, M., Wang, Z., Zhao, S., Wang, J., Zhang, P., Cao, X. 2018. A Novel pathway for High Performance RO Membrane : Preparing Active Layer with Decreased Thickness and Enhanced Compactness by Incorporating Tannic Acid into the Support. *J Memb Sci. 555(March*):157-68. Available from: https://doi.org/10.1016/j.memsci.2018.03.025.

[37] Toncheva, A., Mincheva, R., Kancheva, M., Manolova, N., Rashkov, I., Dubois, P. *et al.* 2016. Antibacterial PLA/PEG Electrospun Fibers: Comparative Study between Grafting and Blending PEG. *Eur Polym J.* 75: 223-33.

[38] Antonacci, P., Chevalier, S., Lee, J., Ge, N., Hinebaugh, J., Yip, R., *et al.* 2016. Balancing Mass Transport Resistance and Membrane Resistance when tailoring Microporous Layer Thickness for Polymer Electrolyte Membrane Fuel Cells Operating at High Current Densities. *Electrochim Acta.* 188: 888-97. DOI: 10.1016/j.electacta.2015.11.115

[39] Abdullah, N., Gohari, R. J., Yusof, N., Ismail, A. F., Juhana, J., Lau, W. J. *et al*. 2016. Polysulfone/hydrous ferric Oxide Ultrafiltration Mixed Matrix Membrane: Preparation, Characterization and Its Adsorptive Removal of Lead (II) from Aqueous Solution. Chem Eng J. 289(II): 28-37. Available from: http://dx.doi.org/10.1016/j.cej.2015.12.081.

[40] Zangeneh, H., Zinatizadeh, A. A., Zinadini, S. 2020. Self-cleaning Properties of L-Histidine Doped TiO2-CdS/PES Nanocomposite Membrane: Fabrication, Characterization and Performance. *Sep Purif Technol.* 240(August 2019): 116591. Available from: https://doi.org/10.1016/j.seppur.2020.116591.

[41] Miller, D. J., Dreyer, D. R., Bielawski, C. W., Paul, D. R., Freeman, B. D. 2017. Surface Modification of Water Purification Membranes. *Angew Chemie - Int Ed.* 56(17): 4662-711.

[42] Jyothi, M. S., Nayak, V., Padaki, M., Balakrishna, R. G., Soontarapa, K. 2015. Aminated Polysulfone/TiO2 Composite Membranes for an Effective Removal of Cr (VI). *Chem Eng J.* (Vi). Available from: http://dx.doi.org/10.1016/j.cej.2015.08.116.

[43] Lufrano, E., Simari, C., Lo Vecchio, C., Aricò, A. S., Baglio, V., Nicotera, I. 2020. Barrier Properties of Sulfonated Polysulfone/Layered Double Hydroxides Nanocomposite Membrane for Direct Methanol Fuel Cell Operating at High Methanol Concentrations. *Int J Hydrogen Energy.* 45(40): 20647-58.

[44] Duan, X., Wang, C., Wang, T., Xie, X., Zhou, X., Ye, Y. 2018. A Polysulfone-based Anion Exchange Membrane for Phosphoric Acid Concentration and Puri Fi Cation by Electro-electrodialysis. *J Memb Sci.* 552*(N*ovember 2017): 86-94. Available from: https://doi.org/10.1016/j.memsci.2018.02.004.

[45] Ma, Y., Dai, J., Wu, L., Fang, G., Guo, Z. 2017. Enhanced Anti-ultraviolet, Anti-fouling and Anti-bacterial Polyelectrolyte Membrane of Polystyrene Grafted with Trimethyl Quaternary Ammonium Salt Modified Lignin. *Polymer* (Guildf) [Internet]. 114: 113-21. Available from: http://dx.doi.org/10.1016/j.polymer. 02.083

[46] Suleman, M. S., Lau, K. K., Yeong, Y. F. 2016. Characterization and Performance Evaluation of PDMS/PSF Membrane for CO_2/CH_4 Separation under the Effect of Swelling. *Procedia Eng*. 148: 176-83. Available from: http://dx.doi.org/10.1016/j.proeng.2016.06.525.